Monatshefte für Chemie 136, 1553–1566 (2005)
DOI 10.1007/s00706-005-0352-5

Monatshefte für Chemie
Chemical Monthly
Printed in Austria

Study on the Kinetics of Non-isothermal Dehydration of Alkaline Earth Metal Selenites

Lyubomir T. Vlaev*, **Maria M. Nikolova,** and **Georgy G. Gospodinov**

Assen Zlatarov University, Bourgas 8010, Bulgaria

Received November 9, 2004; accepted (revised) January 17, 2005
Published online August 10, 2005

Summary. The dehydration kinetics of crystallohydrates of beryllium, magnesium and calcium selenites were studied under non-isothermal conditions. The values of the activation energy of dehydration, the pre-exponential factor in *Arrhenius* equation and the change of entropy for the formation of the activated complex were calculated using the calculation procedure of *Coats* and *Redfern*. Thermal stability and activation energy of dehydration of the crystallohydrates were found to increase by the same order. The relationships observed were interpreted using *Klopman*'s generalized perturbation theory of chemical reactivity. The same theory was applied to explain the differences in the IR spectra of the selenite crystallohydrates studied.

Keywords. Beryllium, magnesium, calcium, strontium and barium selenites; Non-isothermal kinetics of dehydration; Kinetic compensation effect; Generalized perturbation theory; IR-spectroscopy.

Introduction

Within the general tendency of rapid development of many new industries – electronics, telemechanics, and connected with them productions of semiconductors and luminophores [1, 2] – selenium and its compounds became much more significant from scientific and practical points of view. Selenium compounds in oxidation state +4 have versatile practical applications. The salts of the selenium acid – selenites – are used as micro-fertilizers and repellents in agriculture [3, 4], as catalysts in organic synthesis [5], for quantitative determination of some metals forming slightly soluble selenites [6, 7], *etc*. They are precursors for preparation of pure selenides of stoichiometric composition [8, 9], which also possess valuable semiconductor properties. Besides, they are important intermediate products in the technology for production and purification of selenium [10]. Some of them can be found in polymetallic ores as individual minerals [11] but most of them have been synthesized in laboratories only. The selenites are also used as pigments for glasses and enamels [12, 13] and, recently, as antioxidants in medicine.

* Corresponding author. E-mail: vlaev@btu.bg

The crystallohydrates of beryllium and selenium have already been studied and described [15, 16]. The monohydrate and dihydrate of beryllium selenite have been discussed in Ref. [15], the tetrahydrate $BeSeO_3 \cdot 4H_2O$ – in Refs. [15–17]. The authors have shown X-ray diagrams and IR spectra of these compounds.

Opposite to the normal beryllium selenite, magnesium selenite has been more thoroughly studied [18–25]. Preparation and some properties of $MgSeO_3 \cdot 6H_2O$ have been reported in Refs. [19–28]. The crystallohydrate $MgSeO_3 \cdot 2H_2O$ has been studied by chemical and X-ray phase analysis [29]. The normal selenite $MgSeO_3 \cdot 3H_2O$ has been described in Ref. [30]. Its chemical composition was proved by chemical, X-ray phase, and thermal analyses. Later, the field of equilibrium existence of $MgSeO_3 \cdot 6H_2O$ was also reported. Using thermogravimetric analysis, the existence of amorphous anhydrous $MgSeO_3$ was proved and its IR spectra were recorded [31]. Some authors [18, 27] have studied in detail the decomposition of $MgSeO_3 \cdot 6H_2O$ under heating by thermogravimetric and chemical analyses. It was found that the compound lost its water of crystallization within the interval 443–473 K to transform into an X-ray amorphous product. The latter crystallized exothermally at 743 K. The decomposition of the salt to selenium dioxide and metal oxide occurred from 1003 to 1113 K.

Publications [18, 20, 25, 27, 32] described the preparation of normal selenites of calcium ($CaSeO_3 \cdot H_2O$ and $CaSeO_3$) and some of their properties were studied. A detailed study of the system $CaSeO_3$–SeO_2–H_2O was reported in [33]. A solubility isotherm of the system was studied and the fields of equilibrium existence of the phases were found. Thermogravimetric analysis showed that the crystallohydrate dehydrated in the temperature interval 681–761 K and loses 9.59% of its weight in the interval 806–1106 K to transform into crystalline $CaSeO_3$ – (I) or α-$CaSeO_3$. An endothermic effect was observed in the interval 1106–1116 K attributed to recrystallization, with α-$CaSeO_3$ transforming into β-$CaSeO_3$ at temperatures above 1116 K.

Synthesis and properties of strontium and barium selenites were studied and reported in Refs. [18, 20, 25, 27, 32, 34–36]. The following normal selenites were investigated and described: $SrSeO_3 \cdot 3H_2O$, $SrSeO_3$, and $SrSeO_3 \cdot nH_2O$ ($n = 0.6$–1.0); $BaSeO_3 \cdot H_2O$, and $BaSeO_3$. The comprehensive review of *Verma* [37] did not contain dehydration kinetics data for the different crystallohydrates of these selenites.

The aim of the present paper is to study the dehydration kinetics of selenites of alkaline-earth elements under non-isothermal conditions and to interpret the relationships observed in terms of the generalized perturbation theory of chemical reactivity.

Results and Discussion

Figure 1 shows the TG, DTA, and DTG curves of thermal dehydration of $BeSeO_3 \cdot 6H_2O$, $MgSeO_3 \cdot 6H_2O$, and $CaSeO_3 \cdot 2H_2O$.

As can be seen from Fig. 1, the TG curves had two steps, which correspond to two endothermic effects on the DTA curves. It means that the dehydration occurred in two stages. According to the TG curves for $BeSeO_3 \cdot 6H_2O$ and $MgSeO_3 \cdot 6H_2O$, the first step corresponds to the release of 3 mol of water and formation of the corresponding trihydrates. The second step results from the dehydration of the

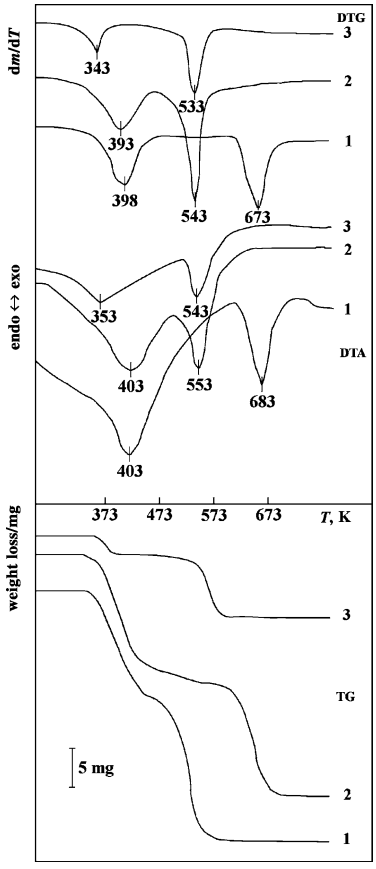

Fig. 1. TG, DTA, and DTG curves of: 1 – $BeSeO_3 \cdot 6H_2O$; 2 – $MgSeO_3 \cdot 6H_2O$; 3 – $CaSeO_3 \cdot 2H_2O$

trihydrates to anhydrous selenites. The first step in the TG curve of $CaSeO_3 \cdot 2H_2O$ corresponds to its dehydration to monohydrate and the second one to dehydration to anhydrous selenite. It means that two structurally and energetically nonequivalent crystal water molecules can be distinguished. This can be rationalized by the structures of magnesium selenite trihydrate and calcium selenite dihydrate shown in Scheme 1 [54].

It is well known [55] that the smaller the cation radius, the higher is its hydration number and the stronger the hydrating molecules are bonded. It means that the maximal amount of crystal water should be expected to decrease from top to bottom of the Periodic table group. Indeed, beryllium and magnesium selenites

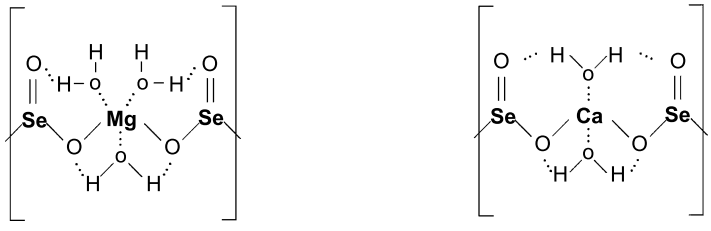

Scheme 1

Table 1. Kinetics parameters of non-isothermal dehydration of some selenite crystallohydrates

Parameter	First stage		
	$BeSeO_3 \cdot 6H_2O$	$MgSeO_3 \cdot 6H_2O$	$CaSeO_3 \cdot 2H_2O$
R^2	0.9985	0.9938	0.9985
n	0.96	0.97	1.01
E/kJ mol^{-1}	44.4	46.9	55.9
A/min^{-1}	4.40×10^5	8.46×10^5	8.98×10^6
Tp/K	398	393	343
$-\Delta S^{\neq}$/J mol^{-1} K^{-1}*	182	176	155
Parameter	Second stage		
	$BeSeO_3 \cdot 6H_2O$	$MgSeO_3 \cdot 6H_2O$	$CaSeO_3 \cdot 2H_2O$
R^2	0.9969	0.9969	0.9994
n	1.02	0.99	0.98
E/kJ mol^{-1}	102.0	159.8	86.8
A/min^{-1}	1.05×10^9	3.38×10^{11}	2.28×10^8
Tp/K	673	543	533
$-\Delta S^{\neq}$/J mol^{-1} K^{-1}*	121	72	132

* $\Delta S^{\neq}$-values are calculated at the corresponding peak temperature T_p

crystallize as hexahydrates while crystallohydrates of barium selenite have not been reported.

Using the data for the corresponding steps of the TG curves for the three selenites, their degrees of dehydration (α) were calculated and, according to the equations presented in Table 1, further calculations were performed to find the equations which give the maximum values of the coefficient of linear regression R^2. Figures 2 and 3 show the linear plots obtained for the kinetic equations, which

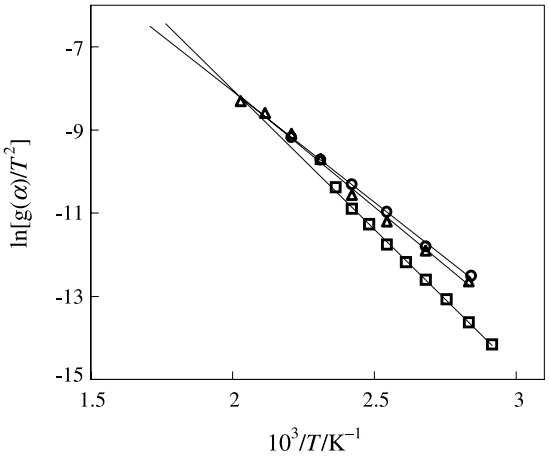

Fig. 2. Kinetics curves of non-isothermal dehydration (first stage) of: 1 – $BeSeO_3 \cdot 6H_2O$; 2 – $MgSeO_3 \cdot 6H_2O$; 3 – $CaSeO_3 \cdot 2H_2O$

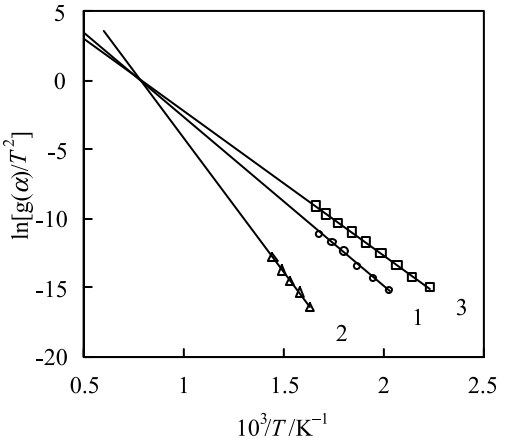

Fig. 3. Kinetics curves of non-isothermal dehydration (second stage) of: 1 – $BeSeO_3 \cdot 6H_2O$; 2 – $MgSeO_3 \cdot 6H_2O$; 3 – $CaSeO_3 \cdot 2H_2O$

gave the maximum values of R^2. In all the cases studied, it turned out to be the so-called mechanism non-invoking equations with values of n, close to unity.

As can be seen from Figs. 2 and 3, the corresponding straight lines crossed at the so-called isokinetic point with accuracies of ± 2 and ± 10 K, respectively. From the first stage it is 494 K, and from the second one 1319 K. The kinetic parameters obtained with this calculation procedure and describing the dehydration of the selenites studied are shown in Table 1.

It can be seen from Table 1 that the kinetic straight lines are characterized by high values of the correlation coefficient R^2 thus, most probably, the kinetic equation is the classic equation for reactions of first order ($n = 1$). Comparing the values of E for the dehydration of $BeSeO_3 \cdot 6H_2O$ and $MgSeO_3 \cdot 6H_2O$ for the two stages, they were found to be higher for the latter. It means that its thermal stability is higher. Taking into account the fact that the dehydration of calcium selenite is connected with a release of only one water molecule whereas the dehydration of beryllium and magnesium produce three water molecules, it may be assumed that the dehydration of calcium selenite is more difficult compared to the others per mol of water. On the other hand, it is well known that the maximal value of the number of molecules of crystallization water decreases from beryllium (hexahydrate) to barium (dehydrate) selenite. Hence, beryllium can form crystallohydrates rich in water but their thermal stability is low. Moving from top to the bottom of the group, the crystallohydrates contain a decreasing amount of water but their thermal stability increases. It is generally accepted [56] that the reactions proceed under diffusion control at values of the activation energy lower than $100\,kJ \cdot mol^{-1}$ whereas at higher values they proceed under kinetic control. Obviously, the release of the first portions of crystallization water occurs as reaction under diffusion control whereas the release of crystallization water during the second stage proceeds as reaction under chemical kinetic control. Such a tendency in the thermal behavior of the crystallohydrates of the selenites of the IIIA group of the Periodic table has been reported in Ref. [57] and described by *Klopman*'s generalized perturbation theory of chemical reactivity [53].

According to the empirical *Pearson*'s order of orbital electronegativity of cations in water [53], the small size of the Be^{2+} ion behaves as ''hard'' acceptor of electrons whereas the large sized Ba^{2+} ion – as ''soft'' acceptor. In this connection, SeO_3^{2-} ion (soft donor of electrons) would form weaker bonds with the beryllium ion and stronger ones with the barium ion. This explains the lower thermal stability of beryllium selenite crystallohydrates and the higher thermal stability of calcium and especially strontium selenite monohydrates. Studying the decomposition kinetics of Group IIA and IIB hydroxides, *L'vov* and *Ugolkov* [58] also observed a tendency of increase of thermal stability and the values of activation energy of the process from top to bottom of the groups. The *E* parameters of the *Arrhenius* equation (in $kJ \cdot mol^{-1}$) are as follows: 124.8 (Be), 166.4

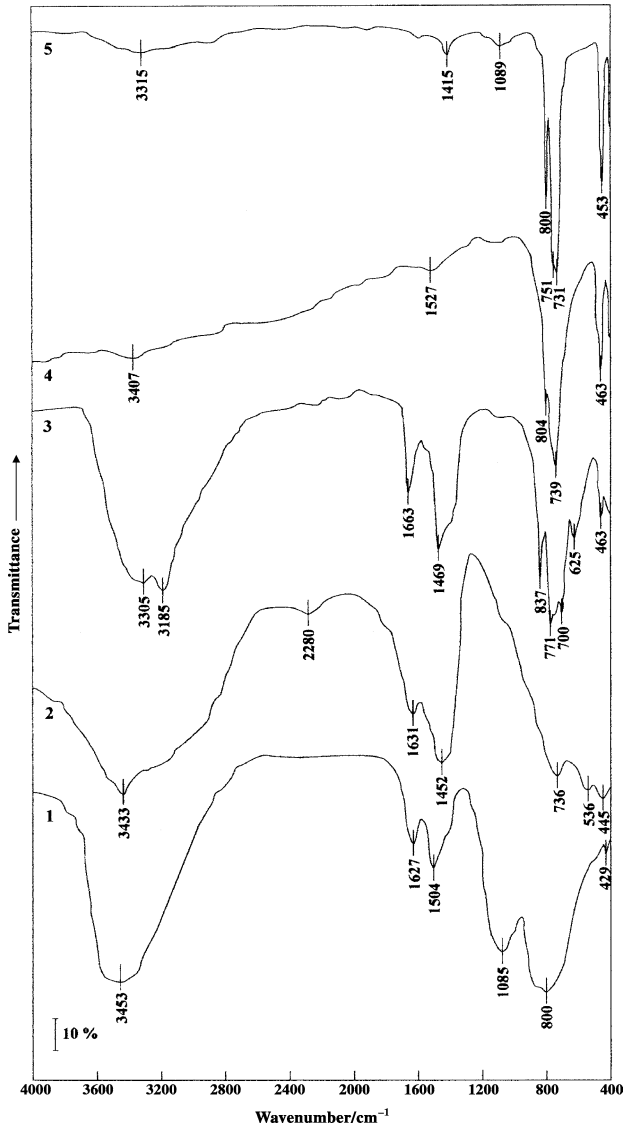

Fig. 4. IR-spectra of: 1 – $BeSeO_3 \cdot 6H_2O$; 2 – $MgSeO_3 \cdot 6H_2O$; 3 – $CaSeO_3 \cdot 2H_2O$; 4 – $SrSeO_3$; 5 – $BaSeO_3$

(Mg), 172.9 (Ca), 181.7 (Sr), 173.4 (Ba), 122.0 (Zn) and 124.7 (Cd). This fact once again confirms the suggestion made by the authors about the existence of a relationship between the thermal stability of compounds and the activation energy of their decomposition under heating and the radius of their ions and their ''hardness'' or ''softness''.

As can be seen from Table 1, the system with a higher entropy change $\Delta S^{\neq}$ will require less energy E for its thermal dehydration [57, 59]. This dependence is more pronounced at the second stage of dehydration.

The IR spectra registered also confirmed the tendency of increase of the crystallohydrates' thermal stability with increase of their cation's radius found (Fig. 4).

Figure 4 shows that the spectra of $BeSeO_3 \cdot 6H_2O$, $MgSeO_3 \cdot 6H_2O$, and $CaSeO_3 \cdot 2H_2O$ in the ranges 3600–3000 and 1650–1300 cm^{-1} contain absorption bands which were not found in the IR spectra of anhydrous $SrSeO_3$ and $BaSeO_3$. The bands with maxima at about 3450 cm^{-1} are due to stretching vibration of the O–H bond whereas these at about 1650–1500 cm^{-1} are due to deformation vibrations of the water [60–64] in the crystallohydrates. The second absorption band is a doublet, which shows that there are two types of crystallization water (see Scheme 1). This was confirmed also by the splitting of the bands at 3305 and 3185 cm^{-1} for $CaSeO_3 \cdot 2H_2O$. Such splitting was not observed for the hexahydrates but the band is much wider. Probably, the large number of molecules masks the split and the band is registered as wide and intensive. It should be noted that the bands corresponding to the deformation vibrations of water molecules shift to higher frequencies from $BeSeO_3 \cdot 6H_2O$ (1504 cm^{-1}) to $CaSeO_3 \cdot 2H_2O$ (1469 cm^{-1}). Since strong interactions between water molecules and cation result in decreased force constants within the bonding of water molecules, the bands are shifted toward lower frequencies. This is an indication that the bond strength of the water molecules in the crystallohydrate increases in the same direction. A series of absorption bands characteristic for selenites were observed in the low frequency part of the spectrum (1100–400 cm^{-1}) [60–64]. Besides, this part of the spectrum becomes more detailed with the decrease of crystallization water. Obviously, it leads to overlapping of some bands so the symmetric and asymmetric stretching vibrations in the selenite anion could not be registered. This was considered to be another confirmation that *Klopman*'s generalized perturbation theory of chemical reactivity explains very well the tendency found in the change of the thermal stability of the selenites studied in relation to their dehydration.

Experimental

Materials

The selenites selected for investigation were synthesized from the following metal salts: beryllium and magnesium sulfates and calcium, strontium, and barium nitrates. All the salts used were at least of 99.9% purity. The sodium selenite was synthesized by the authors from SeO_2 and NaOH with a content of the main component of 99.9%. All metal salts were used as aqueous solutions and mixed in stoichiometric ratios. After precipitation, the selenites were kept in the native solution for 15 days for crystallization. Then, the compounds obtained were separated from the solution and the foreign ions were removed by filtration and washing with distilled water. Further, they were dried at room temperature to constant weight. The selenites were characterized by chemical and X-ray phase

$$A(solid) \rightarrow B(solid) + C(gas)$$

Scheme 2

analyses. The chemical analysis for the metal ions was performed complexometrically at $pH = 10$ with eriochrome black T as indicator [38] whereas the selenite ions were determined both iodometrically and gravimetrically [39]. The X-ray determination was carried out on a URD-6 apparatus (Germany). According to our data obtained from X-ray powder analysis and Ref. [21], $MgSeO_3 \cdot 6H_2O$ crystallizes in the hexagonal system, space group $P6_3/mmc$, with $a = 8.9618$ and $c = 8.9116$ Å. $BeSeO_3 \cdot 6H_2O$ studied also crystallizes in space group $P6_3/mmc$, with $a = 9.0714$ and $c = 8.8824$ Å. $CaSeO_3 \cdot 2H_2O$ crystallizes in the orthorhombic system, space group $Pmmm$, with $a = 10.3463$, $b = 10.1363$, and $c = 9.0182$ Å. The thermogravimetric analysis was carried out on a derivatograph of system F. Paulik – I. Paulik – L. Erdey (MOM, Hungary). Samples of 100 mg were used for the experiments. The TG, TDA, and DTG curves were recorded graphically with 1 mg sensitivity. Alumina was used as a standard reference material. The IR spectra were registered on spectrophotometer Specord – 75 (Carl Zeiss, Germany). For this purpose, 1 mg of the samples was pressed with proper amount of KBr into tablets. The spectra were taken at room temperature.

Since some controversial data have been published on the number of molecules of crystallization water, the crystallohydrates obtained were subjected to precise chemical and thermogravimetric analyses. These compounds were found to be: $BeSeO_3 \cdot 6H_2O$, $MgSeO_3 \cdot 6H_2O$, $CaSeO_3 \cdot 2H_2O$, $SrSeO_3$ and $BaSeO_3$.

Mathematical Background

Dehydration of crystal hydrates is a solid-state process of the type shown in Scheme 2. The kinetics of such reactions is described by various equations taking into account the special features of their mechanisms. The reaction rate can be expressed through the degree of conversion α according to Eq. (1) where m_o, m_f, and m_i are initial, final and current (time t) mass of the sample, respectively.

$$\alpha = \frac{m_o - m_i}{m_o - m_f} \tag{1}$$

Generally, the kinetic equation of the process can be written as shown by Eq. (2) [40].

$$d\alpha/dt = k(T)f(\alpha). \tag{2}$$

The temperature dependence of the rate constant k for the process is described by the *Arrhenius* Eq. (3) where A is the pre-exponential factor, T is the absolute temperature, R is the gas constant, and E is the activation energy.

$$k = A\exp(-E/RT) \tag{3}$$

Substitution of Eq. (3) in Eq. (2) gives Eq. (4).

$$d\alpha/dt = A\exp(-E/RT)f(\alpha). \tag{4}$$

When the temperature increases at a constant rate (Eq. (5)), Eq. (4) can be rearranged to give Eq. (6).

$$dT/dt = q = \text{const}, \tag{5}$$

$$\frac{d\alpha}{dT} = \frac{A}{q}\exp(-E/RT)f(\alpha) \tag{6}$$

The conversion function $f(\alpha)$ for a solid-state reaction depends on the reaction mechanism and can generally be considered to be as shown by Eq. (7) where m, n, and p are empirically obtained exponent factors, one of them always being zero [41].

$$f(\alpha) = \alpha^m(1-\alpha)^n[-\ln(1-\alpha)]^p \tag{7}$$

After substitution in Eq. (6), separation of variables, and integration, Eq. (8) was obtained.

$$\int_0^{\alpha} \frac{d\alpha}{\alpha^m(1-\alpha)^n[-\ln(1-\alpha)]^p} = \frac{A}{q}\int_0^{T} \exp\left(-\frac{E}{RT}\right)dT \tag{8}$$

The solutions of the left hand side integral depend on the explicit expression of the function f(α) and are denoted as g(α). Their algebraic expressions are presented in Table 2.

Table 2. Algebraic expressions of f(α) and g(α) for the kinetic models of solid-state reactions considered in the present work

Symbol	$f(\alpha) = \alpha^m(1-\alpha)^n \times[-\ln(1-\alpha)]^p$	$g(\alpha) = \int_0^{\alpha} \frac{d\alpha}{f(\alpha)} = kt$	Reaction model
1. Chemical decomposition process or mechanism non-invoking equations			
$F_{3/2}$	$(1-\alpha)^{3/2}$	$2[(1-\alpha)^{-1/2}-1]$	Three-halves order kinetics
F_2	$(1-\alpha)^2$	$\alpha/(1-\alpha)$	Second-order kinetics
F_n	$(1-\alpha)^n$	$[1-(1-\alpha)^{1-n}]/(1-n)$	n^{th} order kinetics ($n \neq 1$)
2. Acceleratory rate equations			
$P_{3/2}$	$\alpha^{-1/2}$	$(2/3)\ \alpha^{3/2}$	Power law ($\alpha = kt^{2/3}$)
P_2	$\alpha^{1/2}$	$2\ \alpha^{1/2}$	Power law ($\alpha = kt^2$)
P_3	$\alpha^{2/3}$	$3\ \alpha^{1/3}$	Power law ($\alpha = kt^3$)
P_4	$\alpha^{3/4}$	$4\ \alpha^{1/4}$	Power law ($\alpha = kt^4$)
P_5	α	$\ln\alpha$	Exponential law ($\alpha = 1-\exp(-kt)$)
3. Sigmoid rate equations or random nucleation and subsequent growth			
A_1, F_1	$1-\alpha$	$-\ln(1-\alpha)$	Random nucleation or first order kinetics
$A_{3/2}$	$(1-\alpha)[-\ln(1-\alpha)]^{1/3}$	$(3/2)[-\ln(1-\alpha)]^{2/3}$	*Avrami – Erofe'ev* eq. ($n = 1.5$)
A_2	$(1-\alpha)[-\ln(1-\alpha)]^{1/2}$	$2[-\ln(1-\alpha)]^{1/2}$	*Avrami – Erofe'ev* eq. ($n = 2$)
A_3	$(1-\alpha)[-\ln(1-\alpha)]^{2/3}$	$3[-\ln(1-\alpha)]^{1/3}$	*Avrami – Erofe'ev* eq. ($n = 3$)
A_4	$(1-\alpha)[-\ln(1-\alpha)]^{3/4}$	$4[-\ln(1-\alpha)]^{1/4}$	*Avrami – Erofe'ev* eq. ($n = 4$)
A_u	$\alpha\ (1-\alpha)$	$\ln[\alpha/(1-\alpha)]$	*Prout – Tompkins* eq.
4. Deceleratory rate equations			
4. 1. Phase boundary reaction			
R_1, P_1, F_0	$(1-\alpha)^0$	α	One dimensional advance of the reaction interface, power law ($\alpha = kt$) or zero order kinetics

(*continued*)

Table 2 (*continued*)

Symbol	$f(\alpha)=\alpha^m(1-\alpha)^n \times[-\ln(1-\alpha)]^p$	$g(\alpha)=\int_0^\alpha \frac{d\alpha}{f(\alpha)}=kt$	Reaction model
R_2, $F_{1/2}$	$(1-\alpha)^{1/2}$	$2[1-(1-\alpha)^{1/2}]$	Contracting area (cylindrical symmetry) or one-half order kinetics
R_3, $F_{2/3}$	$(1-\alpha)^{2/3}$	$3[1-(1-\alpha)^{1/3}]$	Contracting volume (spherical symmetry) or two-thirds order kinetics
4.2. Based on the diffusion mechanism			
D_1	$1/\alpha$	$\alpha^2/2$	One dimensional diffusion or parabolic law ($\alpha=kt^{1/2}$)
D_2	$1/-\ln(1-\alpha)$	$\alpha+(1-\alpha)\ln(1-\alpha)$	Two dimensional diffusion (*Valensi* eq.)
D_3	$(1-\alpha)^{2/3}/1-(1-\alpha)^{1/3}$	$(3/2)\ [1-(1-\alpha)^{1/3}]^2$	Three dimensional diffusion (*Jander* eq.)
D_4	$(1-\alpha)^{1/3}/1-(1-\alpha)^{1/3}$	$(3/2)\ [1-(2/3)\ \alpha-(1-\alpha)^{2/3}]$	Three dimensional diffusion (*Ginstling – Brounshtein* eq.)
D_5	$(1-\alpha)^{5/3}/1-(1-\alpha)^{1/3}$	$(3/2)\ [(1-\alpha)^{-1/3}-1]^2$	*Zuravlev-Lesokhin-Tempelman* eq.
D_6	$(1+\alpha)^{2/3}/[(1+\alpha)^{1/3}-1]$	$(3/2)\ [(1+\alpha)^{1/3}-1]^2$	*Komatsu-Uemura* or anti-*Jander* eq.

Several authors [40, 42, 43] suggested different ways to solve the right hand side integral. For the present study, the method of *Coats* and *Redfern* [44] was used. Data from TG and DTG curves in the decomposition range 0.1–0.9 were used to determine the kinetic parameters of the process and mathematical analysis was performed by the integral method of *Coats* and *Redfern*. This method has been successfully used for studies on the kinetics of dehydration and decomposition of different solid substances [40, 42, 43]. The kinetic parameters can be derived using a modified *Coats* and *Redfern* equation (Eq. (9)) where $g(\alpha)$ is a function, the expression of which depends on the kinetic model of the occurring reaction.

$$\ln\frac{g(\alpha)}{T^2}=\ln\frac{AR}{qE}-\frac{E}{RT} \tag{9}$$

If the correct $g(\alpha)$ is used, a plot of $\ln[g(\alpha)/T^2]$ against $1/T$ should give a straight line, from which the values of the activation energy E and the pre-exponential factor A in the *Arrhenius* equation can be calculated. The formal expressions of the functions $g(\alpha)$ depend on the conversion mechanism and its mathematical model [40, 42, 43, 45]. The latter usually represents the limiting stage of the reaction – the chemical reactions, random nucleation and nuclei growth, phase boundary reaction, or diffusion. If the correct $g(\alpha)$ is used, the corresponding linear dependence should give the highest correlation coefficient at the linear regression analysis. Table 2 shows the most common kinetic models and their algebraic expressions [40, 42, 43, 45].

The other kinetic parameters of the process can be calculated using the fundamental theory of the activated complex (transition state) and the *Eyring* equation (Eq. (10)) [46, 47] where χ is the transition

factor, which is unity for monomolecular reactions, k_B is the *Boltzmann* constant, h is the corresponding *Plank* constant, $e = 2.7183$ is the *Neper* number, and $\Delta S^{\neq}$ is the change of entropy for the activated complex formation from the reagent.

$$k = \frac{e\chi k_B T}{h} \exp\left(\frac{\Delta S^{\neq}}{R}\right) \exp\left(-\frac{E}{RT}\right) \tag{10}$$

Taking into account Eq. (10) and the pre-exponential factor from the *Arrhenius* Eq. (3), Eq. (11) is obtained and $\Delta S^{\neq}$ can be calculated according to Eq. (12) where T_p is the peak temperature from the DTG curve.

$$A = \frac{e\chi k_B T}{h} \exp\left(\frac{\Delta S^{\neq}}{R}\right) \tag{11}$$

$$\Delta S^{\neq} = R \ln \frac{Ah}{e\chi k_B T_p} \tag{12}$$

In the kinetic study of the thermal dehydration or decomposition of solids, the determination of the appropriate mechanistic function $g(\alpha)$ is one of the most important subjects. A proper selection of the formal expression of this function should give a linear dependence between $\ln A$ and E. This relation is referred to as the "compensation effect" or "isokinetic effect" or the θ rule [45, 48–52], and may be written as shown by Eq. (13) where k_{iso} is the isokinetic rate constant and T_{iso} is the isokinetic temperature.

$$\ln A = \ln k_{iso} + \frac{E}{RT_{iso}} \tag{13}$$

According to Ref. [49], the value of the rate constant depends mainly on $\Delta H^{\neq}$ at temperatures below T_{iso}, whereas above T_{iso} it depends mainly on $\Delta S^{\neq}$. Various hypotheses have been put forward to elucidate the compensation effect [45, 49]. Two of these hypotheses may be useful for discussion on the applicability of Eq. (13) for some reactions of thermal dissociation. According to one of them, a part of the reaction is a transfer of an electron or a proton by means of the tunnel effect. In this case, a transition factor appears in the formula describing the rate constant. The transition factor χ is described by Eq. (14) [49] where V is the height of the tri-dimensional potential barrier; W is the energy of the tunneling molecule; m is the molecule's mass, and r is the barrier width.

$$\chi = \exp\left\{-\frac{8\pi r}{3h}[2m(V - W)]^{1/2}\right\} \tag{14}$$

Considering Eq. (14), it can be seen that the higher the value of W ($\approx E$), the greater the transition probability and the higher the A value. This hypothesis seems to be valid only for some electron mechanisms and for reactions of protons at low temperatures.

The other hypothesis is based on the assumption that the compensation effect resulting from the reaction acts on active centers of different activation energies according to an exponential distribution.

For the interpretation of the dependencies observed in the change of the kinetic parameters of the selenites studied, the idea suggested by *Klopman* and *Hudson* in their generalized perturbation theory of chemical reactivity [53] was used. It is based on the supposition that the formation of the transition state is brought about by both the mutual perturbation of the molecular orbitals of the two reagents and the electrostatic interaction between the ions, taking into account the influence of the solvent. The relative reactivity of the ions in the solution is assessed by the decrease of energy of the system ΔE. The highest reactivity and, thus, the highest bond strength showed the ions the interaction of which leads to the highest values of ΔE. The basic equation used to determine ΔE for the interaction between the ions is as shown by Eq. (15) [53] where ΔE_{total} is the total change in perturbation energy due to the partial formation of a bond between an anion and cation respectively, q_a and q_c are the total initial charges for anion and cation, R_{ca} is the distance between two ions, ε is related to the local dielectric

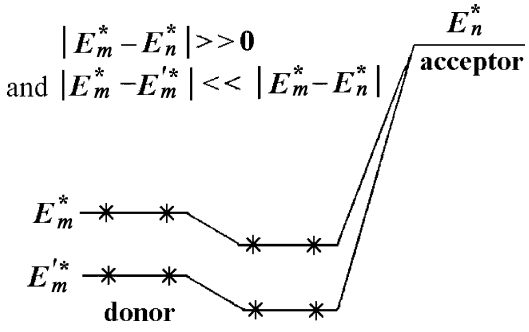

Fig. 5. Charge-controlled effect

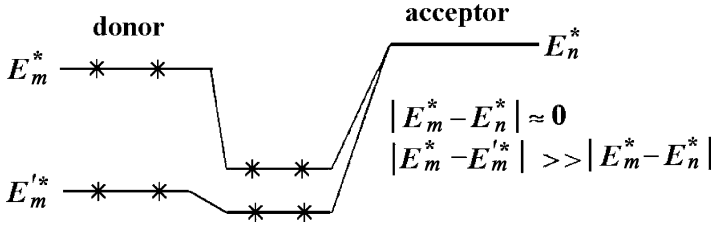

Fig. 6. Orbital-controlled effect

constant of the solvent, $(C_c^m)^2$ and $(C_a^n)^2$ are the frontier electron densities, $\Delta\beta_{ca}^2$ is the change in the resonance integral between the interacting orbitals of anion and cation, $(E_m^* - E_n^*)$ is the difference in energy between the highest occupied orbital of the anion and the lowest empty orbital of the cation.

$$\Delta E_{\text{total}} = \underbrace{-\frac{q_c q_a}{R_{ca}\varepsilon}}_{\substack{\text{electrostatic}\\ \text{term}}} + \underbrace{2\sum_{\text{occ}}(C_c^m)^2 \sum_{\text{unocc}}(C_a^n)^2 \frac{\Delta\beta_{ca}^2}{(E_m^* - E_n^*)_{\text{average}}}}_{\text{covalent term}} \tag{15}$$

When the difference between E_m^* and E_n^* for the frontier orbitals is large, $|E_m^* - E_n^*| \gg 0$, then very little charge transfer occurs (Fig. 5).

In such a case, obviously, the perturbation energy is determined mainly by the total charge of the two ions. Since the electron transfer is quite small, the reaction will be called a charge-controlled reaction. On the other hand, when the two frontier orbitals are degenerate, *i.e.* $|E_m^* - E_n^*| \approx 0$, then, their interaction becomes predominant (Fig. 6).

In this case the electron transfer between them is extensive. Therefore, such reactions will be called orbital-controlled reactions. In this connection, we have established two possible pathways and energetic controls for any couple of ions.

References

[1] Markovskii LYa, Smirnov RI (1959) Izv AN SSSR, Ser Fiz **23**: 1241
[2] Tananaev IV, Volodina AN, Bolshakov NK, Petrov KI (1976) Inorg Mater **12**: 2212
[3] Boling R (1989) American Forest **31**: 326
[4] US Patent No 5340603 (1993)
[5] Pikh ZG, Kosmina II, Samarik VYa, Sheredko AA (1991) Neftekhimiya **31**: 322
[6] Funkoshi O (1935) Bull Chem Soc Japan **10**: 359
[7] Filippova NA, Martynova LA, Savina EV (1960) Zav Lab **26**: 401
[8] Sapozhnikov YuP, Markovskii LYa (1964) Zh Neorg Khim **9**: 849

[9] Savchenko GS, Tananaev IV, Volodina AN (1968) Inorg Mater **4**: 369
[10] Kudryavzev AA (1961) Khimiya i teknologiya selena i tellura. Vyshaya shkola, Moskva
[11] Mandarino JA (1994) Eur J Mineral **6**: 337
[12] Simmingskold B, Johnson BR (1954) Glas Tehn **9**: 131
[13] LaKourse WC (1995) Inst Rev Glass Prod Manuf Technol, London, p 23
[14] Gulya AP, Chova SG, Rudik VF, Biyushkin VI, Antosya BM (1994) Koord Khim **20**: 368
[15] Yanizkii IV, Staschene SS (1985) Zh Neorg Khim **30**(8): 2949
[16] Bäumer U, Boldt K, Engelen B, Müller H, Unterderweide K (1999) Z Anorg Allg Chem **625**: 395
[17] Beresina MI, Pachkovskii VV, Pinaev GF (1972) Zh Neorg Khim **17**: 1795
[18] Nilson FL (1874) Bull Soc Chim Fr **21**: 253
[19] Leshchiskaya ZI, Selivanova NM (1966) Zh Neorg Khim **11**: 260
[20] Chukhlantsev GV (1956) Zh Neorg Khim **1**: 2300
[21] Weiss R (1966) Acta Crystallogr **20**: 533
[22] Simon A, Paetzold R (1960) Z Anorg Allg Chem **303**: 39
[23] Paetzold R, Simon A (1959) Z Anorg Allg Chem **301**: 246
[24] Simon A, Paetzold R (1960) Z Elektrochem Ber Bunsenges Phys Chem **64**: 209
[25] Rocchiccioli CC (1958) C R Acad Sci (Paris) **247**: 1108
[26] Berzelius JJ (1819) Ann Miner **4**: 301
[27] Muspratt JS (1849) J Chem Soc **2**: 52
[28] Boutzoureano B (1889) Ann Chem Phys **18**: 309
[29] Lieder OJ, Gattow G (1967) Naturwissenschaften **34**: 443
[30] Stashene S, Vanisku I (1968) Zh Neorg Khim **31**: 602
[31] Ebert M, Havelicek D (1980) Chem Zvesti **34**: 441
[32] Lenher V, Wechter EJ (1925) J Amer Chem Soc **47**: 1253
[33] Ebert M, Havelicek D (1981) Coll Czech Chem Comm **46**: 1740
[34] Berzelius JJ (1818) Ann Chim Phys **9**: 225
[35] Leshchiskaya ZI, Selivanova NM (1965) Zh Fiz Khim **39**: 2036
[36] Neal L, McCrosky CR (1938) J Amer Chem Soc **60**: 911
[37] Verma VP (1999) Thermochim Acta **327**: 63
[38] Prschibil R (1960) Complecsonii v himicheskom analize. Inostrannaya literature, Moscow
[39] Nazarenko II, Ermakov EI (1977) Analiticheskaia Khimia Selena i Tellura. Nauka, Moscow, pp 5, 59
[40] Orfao JJM, Martins FG (2002) Thermochim Acta **390**: 195
[41] Šestak J, Berggen G (1971) Thermochim Acta **3**: 1
[42] Mamleev V, Bourbigot S, LeBras M, Duquesne S, Šestak J (2000) Phys Chem Chem Phys **2**: 4708
[43] Albano CL, Sciamanna R, Aquino T, Martinez J (2000) European Congress on Computational Methods in Applied Sciences and Engineering. Barcelona, September 2000
[44] Coats AW, Redfern FG (1964) Nature (London) **201**: 68
[45] Agrawal KR (1986) J Thermal Anal **31**: 73
[46] Gerasimov Ya, Dreving V, Eremin E, Kiselev A, Lebedev V, Panchenkov G, Shlygin A (1974) Physical Chemistry, vol. 2. Mir, Moscow
[47] Urzhenko AM, Usherov-Marshak AV (1974) Neorg Mater **10**: 888
[48] Nikolaev AV, Logvinenko VA, Gorbatchov VM, Myachina LI (1974) Thermal Analysis. Proceedings forth ICTA Budapest (ed. by I. Buzas), vol 1, p 47
[49] Zmijewski T, Pysiak J (1974) Thermal Analysis, Proceedings forth ICTA Budapest (ed. by I. Buzas) vol 1, p 205
[50] Koga N, Tanaka H (1988) J Thermal Anal **34**: 177
[51] Vyazovkin SV, Lesnikovich AJ, Romanovsky IS (1988) J Thermal Anal **34**: 609
[52] Tanaka H, Koga N (1988) J Thermal Anal **34**: 685
[53] Klopman G (1974) Chemical Reactivity and Reaction Parts. Wiley, New York

[54] Verma VP, Khushu A (1989) J Thermal Anal **35**: 1989
[55] Engel G, Hertz KG (1968) Ber Bunsenges Phys Chem **72**: 808
[56] Bamford CH, Tipper CFH (1980) Comprehensive Chemical Kinetics, vol 22. Elsevier, Amsterdam
[57] Vlaev LT, Nikolova MM, Gospodinov GG (2004) J Solid State Chem **177**: 2663
[58] L'vov B, Ugolkov V (2004) Thermochim Acta **413**: 7
[59] Vlaev LT, Markovska IG, Lyubchev LA (2004) Oxidation Comm **27**: 444
[60] Makatun VN, Melnikova R Ya, Pechkovskii VV, Afanasev MF (1973) Dokl AN SSSR **213**: 353
[61] Melnikova R Ya, Makatun VN, Pechkovskii VV (1974) Zh Neorg Khim **19**: 1864
[62] Ebert M, Micka Z, Pekova I (1982) Chem Zvesti **30**: 169
[63] Ebert M, Micka Z, Pekova I (1982) Coll Czech Chem Comm **74**: 2069
[64] Gospodinov GG, Sukova LM, Petrov KI (1988) Zh Neorg Khim **33**: 1970